



Controlled assembly of high-order nanoarray metal structures on bulk copper surface by femtosecond laser pulses



Wanwan Qin^a, Jianjun Yang^{a,b,*}

^a Institute of Modern Optics, Nankai University, Tianjin 300071, China

^b Changchun Institute of Optics, Fine Mechanics and Physics, Chinese Academy of Sciences, Changchun 130033, China

ARTICLE INFO

Keywords:

Femtosecond laser
Nanostructures
Metal

ABSTRACT

We report a new one-step maskless method to fabricate high-order nanoarray metal structures comprising periodic grooves and particle chains on a single-crystal Cu surface using femtosecond laser pulses at the central wavelength of 400 nm. Remarkably, when a circularly polarized infrared femtosecond laser pulse (spectrally centered at 800 nm) pre-irradiates the sample surface, the geometric dimensions of the composite structure can be well controlled. With increasing the energy fluence of the infrared laser pulse, both the groove width and particle diameter are observed to reduce, while the measured spacing-to-diameter ratio of the nanoparticles tends to present an increasing tendency. A physical scenario is proposed to elucidate the underlying mechanisms: as the infrared femtosecond laser pulse pre-irradiates the target, the copper surface is triggered to display anomalous transient physical properties, on which the subsequently incident Gaussian blue laser pulse is spatially modulated into fringe-like energy depositions via the excitation of ultrafast surface plasmon. During the following relaxation processes, the periodically heated thin-layer regions can be transferred into the metastable liquid rivulets and then they break up into nanodroplet arrays owing to the modified Rayleigh-like instability. This investigation indicates a simple integrated approach for active designing and large-scale assembly of complexed functional nanostructures on bulk materials.

1. Introduction

Production and engineering of metallic nanostructures is of great interest for many applications, including in plasmonics [1], sensing [2], magnetic recording [3], and catalysts for hydrogen energy [4]. Commonly, several nanofabrication techniques have been already developed, for example, on the uses of photon/charged-beam lithography [5,6], microcontact nano-imprinting [7], and laser directing [8]. Although these top-down approaches can be highly controlled in the creating of nanostructures, they often suffer from high cost, low throughput, or time consuming, thus not suitable for large scale production. In contrast, bottom-up methods which build nanostructures via self-assembly process, are usually characterized by the low cost and a large-area extension but in a weak controllable manner [9]. By combining the advantages of the two fabrication methods, a templated self-organization technique has been reported [10–13], in which the highly ordered arrays of nanoparticles are produced by dewetting of thin metal films on the pre-patterned surfaces via thermal and pulsed laser annealing, and their formation actually depends on both the film thickness and predefined structures [14,15]. Because the

templates often have limitations in material types and structure profiles, integrating such multiple steps (top-down fabrication, metal film deposition, and dewetting process) into a simple industrial process is challenging especially for the emerging field of high-temperature nanophotonics [16]. Therefore, it is highly desirable to develop powerful and reliable techniques for the flexible fabrication of nanostructures on solid bulk targets.

Here we present a new one-step-process strategy by femtosecond laser pulses irradiating the bulk copper surface, to generate the composite nanoscale arrays of metal structures with uniformly distributed particle chains within the periodic grooves. Remarkably, the structure dimensions can be well controlled with the incident time-delayed dual-color femtosecond laser pulses. In physical essence, the self-assembly of such periodic nanostructures is originated from the excitation of surface waves on both the optically excited solid and the metastable liquid materials, namely, ultrafast surface plasmon and modified Rayleigh instability are responsible for the formation of nanoscale groove and particle arrays, respectively.

* Corresponding author at: Institute of Modern Optics, Nankai University, Tianjin 300071, China.
E-mail address: jjyang@nankai.edu.cn (J. Yang).

<http://dx.doi.org/10.1016/j.susc.2017.03.005>

Received 25 October 2016; Received in revised form 27 February 2017; Accepted 4 March 2017

Available online 06 March 2017

0039-6028/ © 2017 Elsevier B.V. All rights reserved.

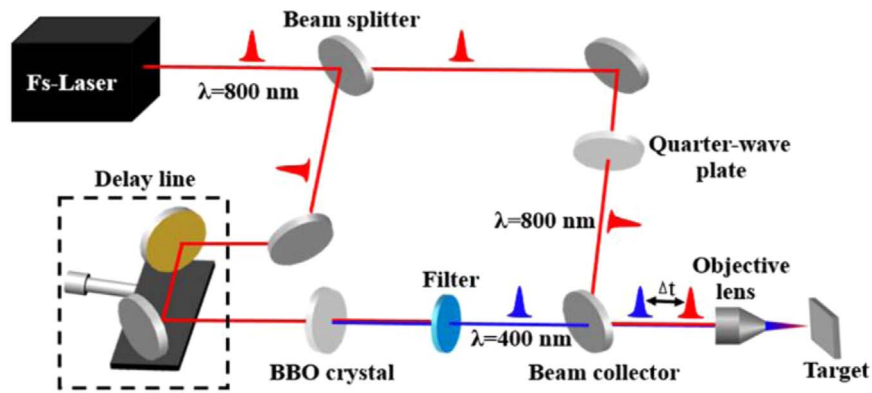


Fig. 1. A schematic diagram of the experimental setup for one-step assembly of high-order nanoarray metal structures on bulk copper surfaces by femtosecond laser pulses.

2. Experimental methods

A schematic diagram of our experimental setup is shown in Fig. 1, where a chirped-pulse amplification of Ti: sapphire laser system (Spectra Physics HP-Spitfire 50) was adopted as a light source, and it delivers linearly polarized 50 fs laser pulse trains at a repetition rate of 1 kHz with the central wavelength $\lambda=800$ nm. The output laser pulse was then split into two beams with a conventional Michelson interferometer, in one arm of which the laser is frequency-doubled by a beta-barium-borate (BBO) crystal and spectrally filtered to the central wavelength of $\lambda=400$ nm, while in another arm the laser is transformed into a circular polarization state via a quarter-wave plate. After passing a beam collector, the two-color femtosecond laser pulses were spatially overlapped into a collinear propagation and focused by an objective lens ($4\times$, N. A=0.1) at normal incidence to the polished surface of a single-crystal Cu plate $\langle 110 \rangle$ (1 mm thickness), which was fixed on a three-dimensional (x-y-z) translation stage (New Port UTM100 PPE1). The roughness (Ra) of the polished Cu surface is less than 5 nm. To avoid serious ablation damages, the sample surface was placed about 400 μm away before the focus, where the laser spot exhibits a Gaussian fluence distribution with a $(1/e^2)$ diameter of approximately 40 μm . The experiment was carried out with a line-scribing method at a scanning speed of 0.1 mm s^{-1} under the fixed irradiation of the laser pulses, resulting in 800 partially overlapped pulses within a beam spot. A temporal delay Δt between the two-color laser beams was able to adjust within a range of 0–140 ps via a high precision optical delay line. Positive time delays indicate the arrival of infrared laser pulse prior to the blue one. The laser energy in each interferometer arm was individually controlled via the neutral attenuators.

3. Results and discussion

First, a single blue femtosecond laser beam of the linear polarization was only used to irradiate the sample by shading the optical path of infrared laser beam in the interferometer, and the obtained morphologies of the laser irradiated surface are displayed in Fig. 2 for two different energy fluences of $F_{\text{blue}}=0.059$ J cm^{-2} and 0.1 J cm^{-2} (It is noted here that the measured threshold fluence for the single-pulse ablation of the polished Cu surface was 0.16 ± 0.02 J cm^{-2}). Clearly, they present a fascinating composite nanostructure: Besides a typical pattern of the periodic grating oriented perpendicular to the laser polarization, a linear row of tiny grains appears to distribute within each grating valley region. Their zoom-in pictures demonstrate that the massive particles, like condensed droplets of the molten material, have nearly smooth round profiles and line up regularly along the groove direction. Under conditions of the two different laser fluences, the available groove periodicity is $\Lambda_g=275.5 \pm 12.1$ nm and 268.7 ± 12.8 nm, much smaller than the incident laser wavelength of 400 nm, and the groove width approximates 95.7 ± 6.8 nm and 114.3

± 13.7 nm, respectively. On the other hand, the measured average particle spacing is $\Lambda_p=181.8 \pm 20.5$ nm and 201.1 ± 18.7 nm, and the particle diameter is about $d=111.8 \pm 17.8$ nm and 132.1 ± 12.3 nm, respectively. The results are much different from those of the previous study on the silicon surface [17], wherein the observed nanoholes present empty cavity profiles, in particular, the distance between the two neighboring nanoholes was measured to be ~ 0.72 μm and the nanohole chains were separated by ~ 2.0 μm . Actually, such hybrid periodic surface structures, also the so-called high-order nanoarray metal structures on the copper surface, can be extended into a large two-dimensional (2D) areas through the sample scanning with other higher laser fluences even up to $F_{\text{blue}}=0.139$ J cm^{-2} .

In order to exploit transient physical properties of the metal for manipulating laser processing results, we began to introduce a circularly polarized infrared femtosecond laser pulse before the blue laser pulse reach the target. The temporal delay between the two-color laser pulses was $\Delta t=+28$ ps and the sample scanning was kept at the speed of 0.1 mm s^{-1} . The infrared laser fluence was selected so delicately that its individual irradiation cannot generate any periodic surface structures. Fig. 3 shows the surface structures obtained by two-color femtosecond laser pulses with variable energy fluences. Compared with the above experiment with the single blue femtosecond laser beam, the laser exposed surfaces by two-color beams can also provide the nanoscale periodic groove-particle composite structures. Under such circumstances, however, the top-view profiles of the nanoparticles located in the grating valley regions become more circular in accompany with the decreasing in either the diameter d or the spacing Λ_p . Moreover, the groove width turns to be narrower. In other words, a pre-incident infrared laser pulse enables to modify the formation of the high-order periodic nanostructures on the copper surface.

To quantitatively evaluate the effects of the pre-incident infrared femtosecond laser pulse, we summarize the measured data of the surface structures in Fig. 3. As shown in Fig. 4(a), for a given energy fluence of the blue femtosecond laser pulse, the available groove width appears to reduce with gradual increasing the infrared laser fluence within a range of 0–0.13 J cm^{-2} , in sharp contrast to the usual expectation of larger interaction regions for the increased dose of the laser exposure [18]. For instance, at $F_{\text{blue}}=0.1$ J cm^{-2} , the groove width, being about 114.3 nm without the infrared laser pre-irradiation, violently decreases down to only about 59.1 nm at $F_{\text{infrared}}=0.08$ J cm^{-2} . This result indicates a new potential method for the nanoscale processing metals with double time-delayed femtosecond laser pulses. On the other hand, for a given energy fluence of the pre-incident infrared laser pulse, the groove width is likely to enlarge with higher fluences of the blue laser. Fig. 4(b) illustrates the variations of the particle diameter as a function of the pre-incident infrared laser fluence. It is revealed that the diameter of the particles resting in the valley regions decreases with higher fluences of the pre-incident

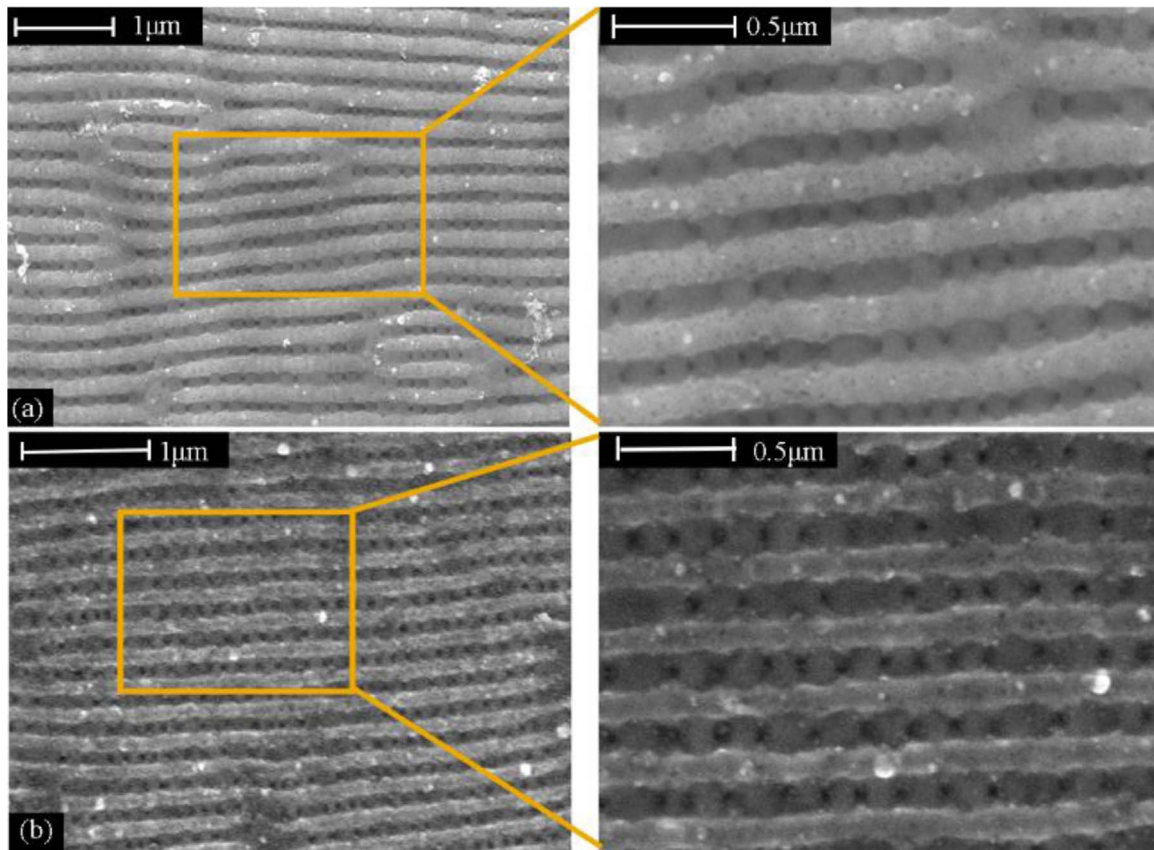


Fig. 2. Scanning electron microscopy (SEM) images of the high-order nanoarray metal structures on the bulk copper surfaces with only irradiation of 400 nm femtosecond laser pulses at two different energy fluences. (a) $F_{\text{blue}}=0.059 \text{ J cm}^{-2}$; (b) $F_{\text{blue}}=0.1 \text{ J cm}^{-2}$.

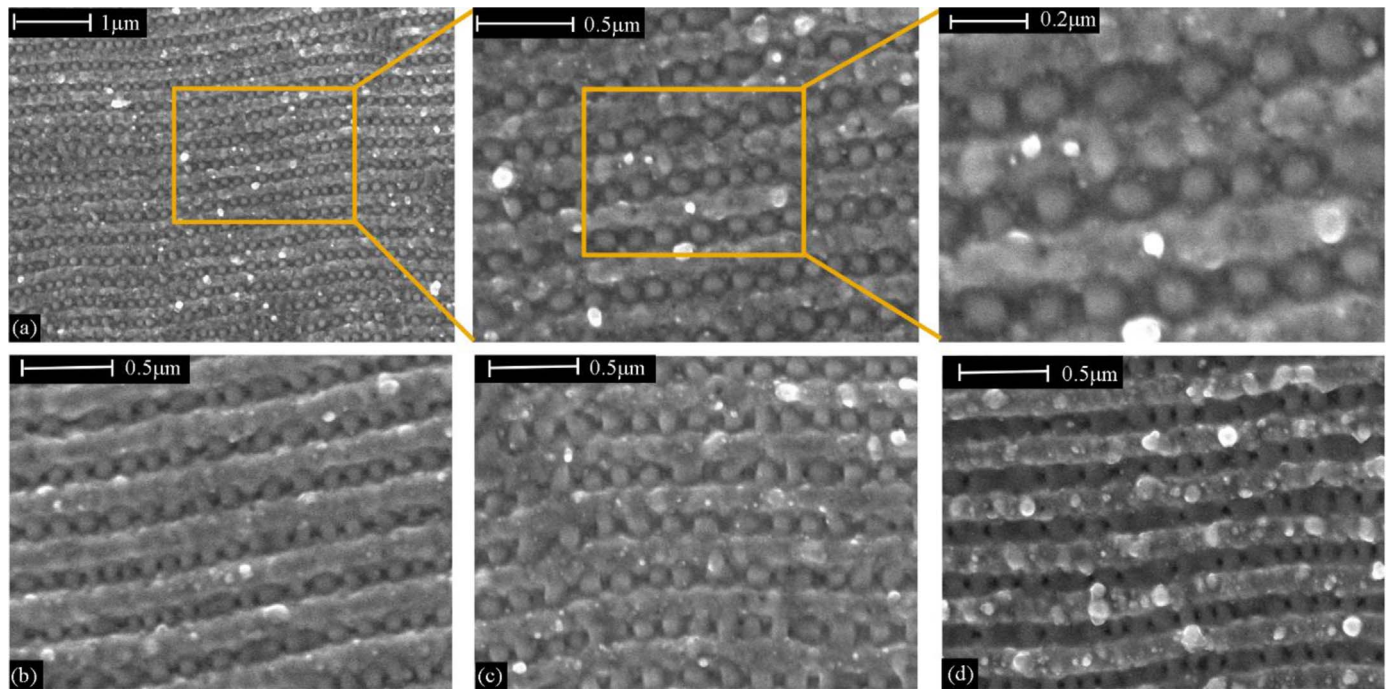


Fig. 3. SEM images of the high-order nanoarray metal structures formed on the bulk copper surfaces with collinear irradiation of two-color time-delayed femtosecond laser pulses, where the energy fluences of both the infrared (800 nm) and the blue (400 nm) laser beams are varied. (a) $F_{\text{infrared}}=0.04 \text{ J cm}^{-2}$ and $F_{\text{blue}}=0.1 \text{ J cm}^{-2}$; (b) $F_{\text{infrared}}=0.02 \text{ J cm}^{-2}$ and $F_{\text{blue}}=0.09 \text{ J cm}^{-2}$; (c) $F_{\text{infrared}}=0.06 \text{ J cm}^{-2}$ and $F_{\text{blue}}=0.1 \text{ J cm}^{-2}$; (d) $F_{\text{infrared}}=0.02 \text{ J cm}^{-2}$ and $F_{\text{blue}}=0.12 \text{ J cm}^{-2}$.

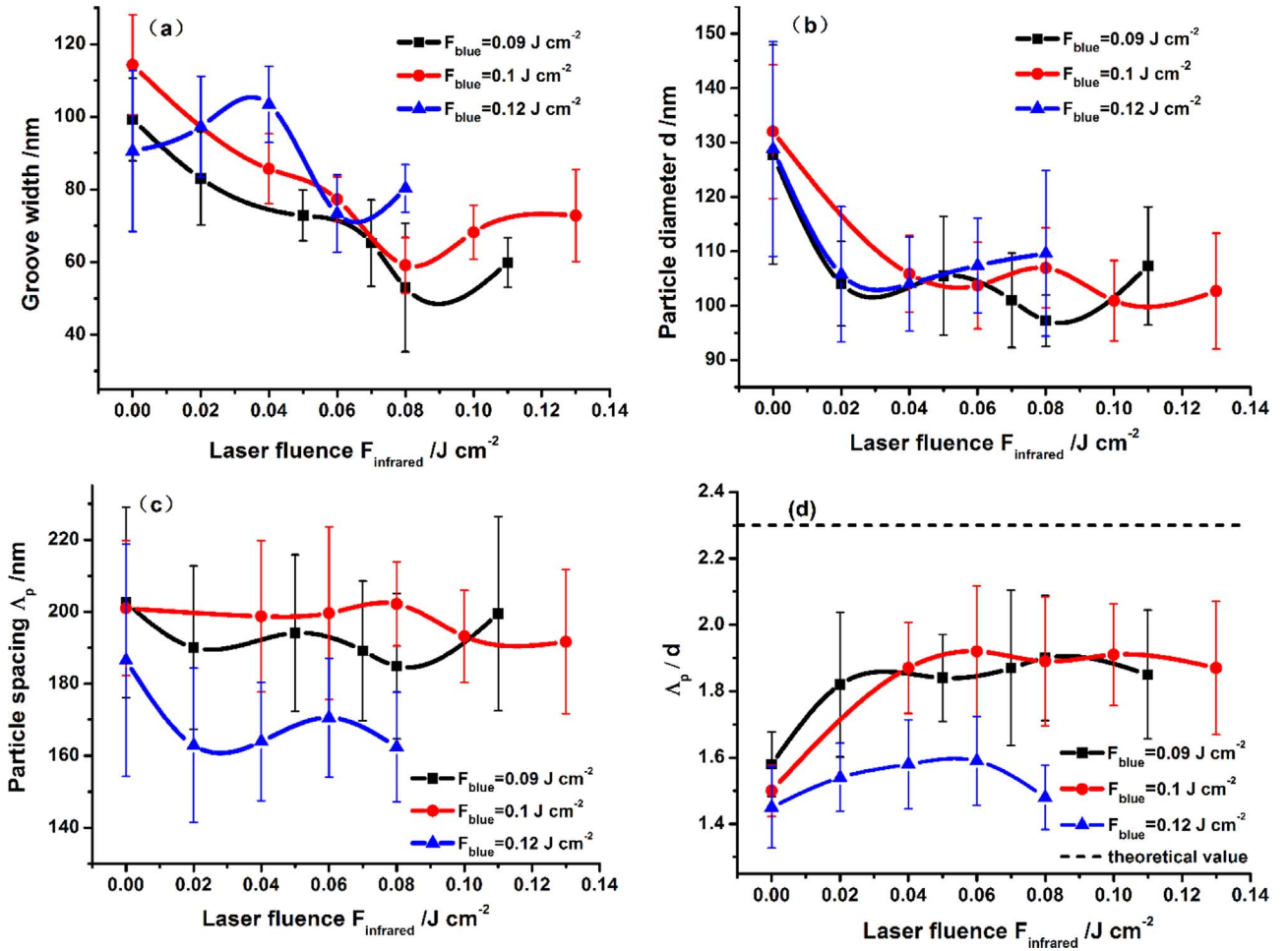


Fig. 4. Measured variations of the geometric dimensions of the high-order nanoarray metal structures for several different energy fluences of both the infrared and the blue laser pulses. (a) Groove width; (b) Particle diameter d ; (c) Particle spacing Λ_p ; (d) Spacing-to-diameter ratio of the nanoparticles Λ_p/d .

infrared laser but increases with larger fluences of the blue laser pulse. From Fig. 4(c), we can find that the particle spacing is almost unaffected by the pre-incident infrared laser fluence, but it can be modulated by the delayed incident blue laser fluence. Furthermore, a ratio of the particle spacing to its diameter, Λ_p/d , is also calculated for the above situations, as shown in Fig. 4(d). Clearly, without irradiation of pre-incident infrared laser pulse, the spacing-to-diameter ratio becomes larger for smaller blue laser fluences; while under the conditions of pre-incident infrared laser fluence, the variations of the obtained ratios display increasing tendencies. The higher the infrared laser fluence or the smaller the blue laser fluence, the larger the Λ_p/d ratio becomes.

A physical scenario for the formation of the high-order nanoarray metal structures upon femtosecond laser irradiating the copper surface is proposed as follows: For the irradiation of a single-beam linearly polarized blue femtosecond laser pulses, ultrafast surface plasmon is firstly excited on the solid metal target, and its subsequent optical interference with the incident light leads to the intensity fringes. Therefore, the material surface is in fact treated by a spatially periodic distribution of the laser energy sources to generate an array of nanoscale thin-layer strip-like heated regions, with orientation perpendicular to the direction of the laser linear polarization. The spatial periodicity Λ_g is equal to the surface plasmon wavelength, which can be described by [19,20],

$$\Lambda_g = \lambda_{\text{laser}} \sqrt{(\epsilon_m + 1)/\epsilon_m} \quad (1)$$

where λ_{laser} is the incident laser wavelength, and ϵ_m is a dielectric constant of the copper material. Moreover, due to the incident small laser energy, the width of each heated region can be much less than the periodicity of the strip arrays, i.e., approximating 100 nm. When the lattice temperatures of these thermally heated regions increase up to the melting point, the straight edged thin-layer strips rapidly transforms, by liquid phase retraction, into the nanoscale rivulet morphology or semi-cylindrical “nanowire” geometry. For a substrate-supported liquid rivulet, a modified Rayleigh-Plateau instability induces surface perturbations to result in the breakup of these nanowires into periodic nanodroplets, which eventually re-solidify as a chain of nanoparticles [21]. With this physical model, it is well understood why the nanoparticles are periodically formed in the valley (concave) rather than on the ridge (convex) regions of the grating structures, with spatial alignments along the groove direction.

For the irradiation with two-color femtosecond laser pulses, the physical processes of developing the high-order nanoarray metal structures are shown in Fig. 5. As the circularly polarized infrared femtosecond laser pulse pre-irradiates the target, the material surface is optically excited to increase the temperatures of both electrons and lattice, displaying anomalous transient physical properties [Fig. 5(a)]. For example, the electron heat conductivity gradually diminishes with increasing the lattice temperature [22]. Thus, at the time delay of 28 ps, close to the characteristic time of electron-lattice coupling, the heat conductivity of the electrons is most likely to reduce. When the delayed blue femtosecond laser pulse strikes the sample, its Gaussian intensity profile is re-distributed into the nanoscale periodic energy depositions

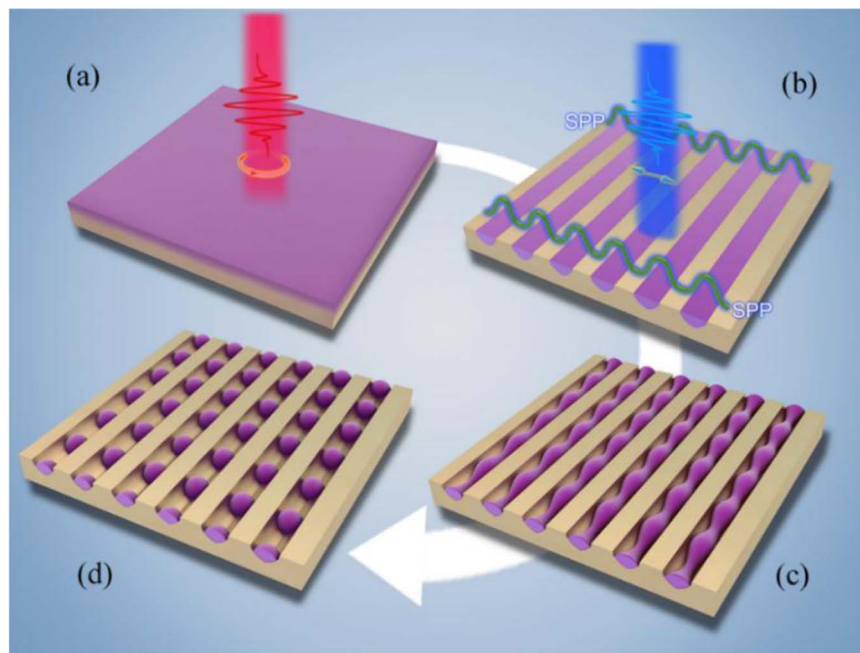


Fig. 5. A proposed physical scenario for the controlled assembly of high-order nanoarray metal structures on the bulk copper surfaces by two-color femtosecond laser pulses.

by the excitation of surface plasmon on the solid target [Fig. 5(b)]. As mentioned in the above experiment with the single-beam blue femtosecond laser pulses, the periodic surface regions are then transiently melted into the thin-layer nanoscale rivulets supported on the bulk substrate, the destabilization of which begins with the growth of the thermal perturbation modes on the liquid surfaces [Fig. 5(c)], *i.e.*, the Rayleigh-like instability occurs. Finally, each liquid rivulet morphology is fragmented into a linear nanoparticle array [Fig. 5(d)]. Because the pre-incident infrared laser pulse transiently decreases the heat conductivity of the sample, the absorbed blue laser energy within each laser-exposed region tends to have an enhanced spatial confinement. As a result, the resultant ablation grooves can present decreasing widths with larger infrared laser fluences, especially for the blue laser fluence of $F_{\text{blue}} < 0.12 \text{ J cm}^{-2}$. However, at the higher blue laser energy of $F_{\text{blue}} = 0.12 \text{ J cm}^{-2}$, the thermal diffusion becomes pronounced with more absorbed energy and leads to the larger groove widths. Under such circumstance, if the infrared laser fluence F_{infrared} increases, the reduced heat conductivity is ready to shrink the groove widths. Moreover, the absorbed energy of the pre-incident infrared laser pulse can also help to raise the periodic nanoscale strip regions into higher temperatures, which eventually decreases the particle diameter.

On the other hand, the elevated temperature by the pre-pulse irradiation can also lower the electrical conductivity of the material via reducing the collision time between the electron [23], resulting in a larger optical penetration depth for the delayed incident blue femtosecond laser pulse. This consequently increases the thickness of the heat-affected regions and makes the volume of the liquid rivulet almost unchanged with increasing the infrared laser fluence, or the radius of the effective liquid cylinder becomes almost constant to maintain the particle spacing. Notably, for a free-standing Rayleigh-Plateau jet with cylindrical geometry, the spacing-to-diameter ratio of the nanoparticles is predicted to be $\Lambda_p/d = 2.3$ [24], as described by a dashed line in Fig. 4(d). However, our observed spacing-to-diameter ratios for the nanoparticles in the valley regions have relatively smaller values. The origin for this discrepancy could be because of the following things: (i) the periodically heated strips or the liquid rivulets are not perfect cylinders; (ii) the fragmentation process of the rivulets is influenced by the metallic substrate and walls. At each given blue laser fluence, the slow rising tendency of the ratio Λ_p/d suggests that both the morphol-

ogy and hydrodynamic property of the liquid rivulet have been modulated gradually with higher pre-irradiation laser fluences.

In addition, we have also carried out the experiments at different time delays between the two-color fs laser pulses within a range of 10–90 ps, where the two laser energy fluences are given by $F_{\text{infrared}} = 0.059 \text{ J cm}^{-2}$ and $F_{\text{blue}} = 0.039 \text{ J cm}^{-2}$, respectively, and some typical SEM images are shown in Fig. 6. Clearly, it is found that both the diameter and the number of the nanoparticles tend to decrease with increasing the time delay between two-color fs laser pulses, which suggests the important role of the relaxation of the transient properties excited by the pre-incident infrared femtosecond laser pulse. These phenomena can also provide further supports for our theory.

4. Conclusions

In summary, we have introduced a one-step method that allow one to produce high-order nanoscale groove-particle structures on the solid copper surfaces with irradiation of 400 nm blue femtosecond laser pulses. The use of flat bulk substrates with neither pre-templates nor thin-film depositions considerably simplifies the nanofabrication process. It is suggested that the formation of the periodic groove array is originated from the ultrafast plasmon excitation on the solid-air surface and its subsequent interference with the light leads to the periodic patterns of the nanoscale thin-layer strips; when these strips are transiently heated into metastable liquid rivulets, the Rayleigh-like instability occurs due to the growth of thermal fluctuations on the liquid-air surface, resulting in their ordered rupture into the nanoparticles along the groove direction. Moreover, we have revealed that the self-assembly of the surface nanostructures can be controlled with the pre-irradiation of the infrared femtosecond laser pulse, which actually modifies the transient optical properties of the sample surface.

Notably, in our experiments the confinement of material dewetting process is based on the transient fringes induced by the surface plasmon, in sharp contrast to the conventional layered systems with substantially constructed surface morphologies by top-down methods. In other words, a big advantage of our method is that the multiple macroscopic procedures for the fabrication of nanoscale composite structures are self-integrated microscopically with the help of transient physical effects originating from the femtosecond laser-metal interac-

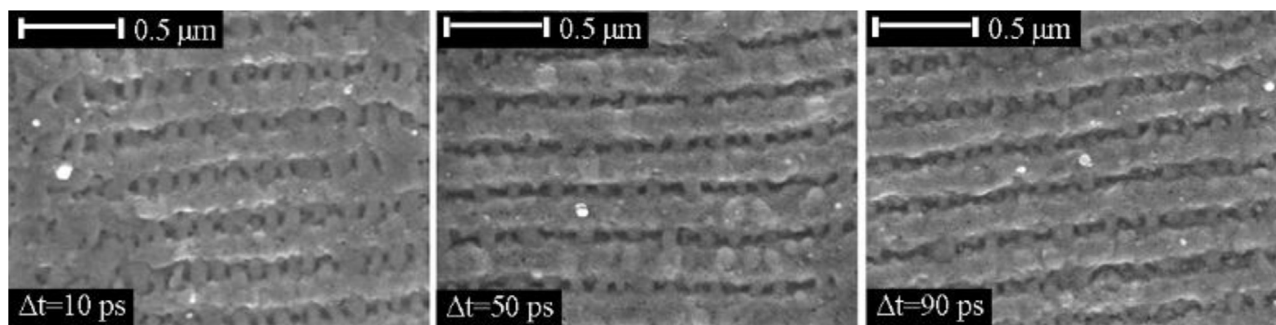


Fig. 6. SEM images of the high-order nanoarray metal structures formed on the bulk copper surfaces with collinear irradiation of two-color femtosecond laser pulses at variable time delays of 10 ps, 50 ps and 90 ps.

tion. Furthermore, the direct writing of such hybrid metal nanoarray surface structures can be flexibly extended into large areas using a broad beam irradiation. We believe that this newly observed phenomenon will stimulate the investigations on versatile nanofabrication process of the femtosecond laser pulses especially with exploiting transient physical properties of materials.

Acknowledgments

We acknowledge financial supports from National Natural Science Foundation of China (11274184, 11674178), Natural Science Foundation of Tianjin (12JCZDJC20200) and the Research Fund for the Doctoral Program of Higher Education of China (20120031110032).

References

- [1] S.A. Maier, M.L. Brongersma, P.G. Kik, S. Meltzer, A.A.G. Requicha, H.A. Atwater, Plasmonics—a route to nanoscale optical devices, *Adv. Mater.* 13 (2001) 1501–1505.
- [2] A.I. Kuznetsov, A.B. Evlyukhin, M.R. Goncalves, C. Reinhardt, A. Koroleva, M.L. Arnedillo, R. Kiyari, O. Marti, B.N. Chichkov, Laser fabrication of large-scale nanoparticle arrays for sensing applications, *ACS Nano* 5 (2011) 4843–4849.
- [3] H.-J. Freund, Clusters and islands on oxides: from catalysis via electronics and magnetism to optics, *Surf. Sci.* 500 (2002) 271–299.
- [4] U. Sahaym, M.G. Norton, Advances in the application of nanotechnology in enabling a ‘hydrogen economy’, *J. Mater. Sci.* 43 (2008) 5395–5429.
- [5] H.H. Solak, Y. Ekinci, P. Käser, S. Park, Photon-beam lithography reaches 12.5 nm half-pitch resolution, *J. Vac. Sci. Technol. B* 25 (2007) 91–95.
- [6] S.Y. Chou, M. Wei, P.R. Krauss, P.B. Fischer, Study of nanoscale magnetic structures fabricated using electron-beam lithography and quantum magnetic disk, *J. Vac. Sci. Technol. B* 12 (1994) 3695–3698.
- [7] Y. Xia, J.A. Rogers, K.E. Paul, G.M. Whitesides, Unconventional methods for fabricating and patterning nanostructures, *Chem. Rev.* 99 (1999) 1823–1848.
- [8] J.P. McDonald, V.R. Mistry, K.E. Ray, S.M. Yalisove, Femtosecond pulsed laser direct write production of nano- and microfluidic channels, *Appl. Phys. Lett.* 88 (2006) 183113.
- [9] H.M. van Driel, J.E. Sipe, J.F. Young, Laser-induced periodic surface structure on solids: a universal phenomenon, *Phys. Rev. Lett.* 49 (1982) 1955–1959.
- [10] T.W.H. Oates, A. Keller, S. Noda, S. Fafsko, Self-organized metallic nanoparticle and nanowire arrays from ion-sputtered silicon templates, *Appl. Phys. Lett.* 93 (2008) 063106.
- [11] J. Basu, C.B. Carter, R. Divakar, B. Mukherjee, N. Ravishanker, Nanopatterning by solid-state dewetting on reconstructed ceramic surfaces, *Appl. Phys. Lett.* 94 (2009) 171114.
- [12] J.D. Fowlkes, Y. Wu, P.D. Rack, Directed assembly of bimetallic nanoparticles by pulsed-laser-induced dewetting: a unique time and length scale regime, *ACS Appl. Mat. Interfaces* 2 (2010) 2153–2161.
- [13] J.D. Fowlkes, L. Kondic, J. Diez, Y. Wu, P.D. Rack, Self-assembly versus directed assembly of nanoparticles via pulsed laser induced dewetting of patterned metal films, *Nano Lett.* 11 (2011) 2478–2485.
- [14] H. Krishna, R. Sachan, J. Strader, C. Favazza, M. Khenner, R. Kalyanaraman, Thickness-dependent spontaneous dewetting morphology of ultrathin Ag films, *Nanotechnology* 21 (2010) 155601.
- [15] Q. Xia, S.Y. Chou, The fabrication of periodic metal nanodot arrays through pulsed laser melting induced fragmentation of metal nanogratings, *Nanotechnology* 20 (2009) 285310.
- [16] V. Rinnerbauer, S. Ndao, Y.X. Yeng, J.J. Senkevich, K.F. Jensen, J.D. Joannopoulos, M. Soljačić, I. Celanovic, R.D. Geil, Large-area fabrication of high aspect ratio tantalum photonic crystals for hightemperature selective emitters, *J. Vac. Sci. Technol. B* 31 (2013) 011802.
- [17] C.Y. Zhang, J.W. Yao, H.Y. Liu, Q.F. Dai, L.J. Wu, S. Lan, V.A. Trofimov, T.M. Lysak, Colorizing silicon surface with regular nanohole arrays induced by femtosecond laser pulses, *Opt. Lett.* 37 (2012) 1106–1108.
- [18] S. Sakabe, M. Hashida, S. Tokita, S. Namba, K. Okamuro, Mechanism for self-formation of periodic grating structures on a metal surface by a femtosecond laser pulse, *Phys. Rev. B* 79 (2009) 033409.
- [19] R. Raether, *Surface Plasmons on Smooth and Rough Surfaces and on Gratings*, First ed., Springer, Berlin, 1988.
- [20] W.L. Barnes, Surface plasmon-polariton length scales: a route to sub-wavelength optics, *J. Opt. A: Pure Appl. Opt.* 8 (2006) S87–S93.
- [21] J. Fowlkes, S. Horton, M. Fuentes-Cabrera, P.D. Rack, Signatures of the Rayleigh-Plateau instability revealed by imposing synthetic perturbations on nanometer-sized liquid metals on substrates, *Angew. Chem. Int. Ed.* 51 (2012) 8768–8772.
- [22] B.H. Christensen, K. Vestentoft, P. Balling, Short-pulse ablation rates and the two-temperature model, *Appl. Surf. Sci.* 253 (2007) 6347–6352.
- [23] K.Y. Kim, B. Yellampalle, J.H. Glowina, A.J. Taylor, G. Rodriguez, Measurements of terahertz electrical conductivity of intense laser-heated dense aluminum plasmas, *Phys. Rev. Lett.* 100 (2008) 135002.
- [24] M.E. Toimil Molaes, A.G. Balogh, T.W. Cornelius, R. Neumann, C. Trautmann, Fragmentation of nanowires driven by Rayleigh instability, *Appl. Phys. Lett.* 85 (2004) 5337–5339.